Journal of Physiology (1993), **469**, *pp.* 245–273
With 8 figures
Printed in Great Britain

MOBILE AND IMMOBILE CALCIUM BUFFERS IN BOVINE ADRENAL CHROMAFFIN CELLS

BY ZHUAN ZHOU* AND ERWIN NEHER

From the Max-Planck-Institut für biophysikalische Chemie, D-3400 Göttingen, FRG

(*Received 17 November 1992*)

SUMMARY

1. The calcium binding capacity (κ_S) of bovine chromaffin cells preloaded with fura-2 was measured during nystatin-perforated-patch recordings.

2. Subsequently, the perforated patch was ruptured to obtain a whole-cell recording situation, and the time course of κ_S was monitored during periods of up to one hour.

3. No rapid change (within 10–20 s) of κ_S was observed upon transition to whole-cell recording, as would be expected, if highly mobile organic anions contributed significantly to calcium buffering. However, approximately half of the cells investigated displayed a drop in κ_S within 2–5 min, indicative of the loss of soluble Ca^{2+} binding proteins in the range of 7–20 kDa.

4. The average Ca^{2+} binding capacity (differential ratio of bound calcium over free calcium) was 9 ± 7 (mean $\pm$ S.E.M.) for the poorly mobile component and 31 ± 10 for the fixed component. It was concluded that a contribution of 7 from highly mobile buffer would have been detected, if present. Thus, this value can be considered as an upper bound to highly mobile Ca^{2+} buffer.

5. Both mobile and fixed calcium binding capacity appeared to have relatively low Ca^{2+} affinity, since κ_S did not change in the range of Ca^{2+} concentrations between 0·1 and 3 μM.

6. It was found that cellular autofluorescence and contributions to fluorescence of non-hydrolysed or compartmentalized dye contribute a serious error in estimation of κ_S. 'Balanced loading', a degree of fura-2 loading such that the calcium binding capacity of fura-2 equals cellular calcium binding capacity, minimizes these errors. Also, changes in κ_S at the transition from perforated-patch to whole-cell recording can be most faithfully recorded for similar degrees of loading in both situations.

7. Nystatin was found unable to make pores from inside of the plasma membrane of chromaffin cells. With careful preparation and storage the diluted nystatin solution maintained its high activity of membrane perforation for more than one week.

8. An equation for the effective diffusion constant for total cytoplasmic calcium, D'_{Ca}, was derived, which takes into account fixed buffer and poorly mobile buffer as determined, as well as calcium bound to fura-2 and some highly mobile buffers.

* Present address: Department of Medicine, Renal Division, Jewish Hospital, 216 S. Kingshighway, St Louis, MO 63110, USA.

MS 1913

9. It was concluded that even for fura-2 concentrations as small as 50 μM, the dye and possibly some immeasurable contribution of highly mobile buffer dominate the diffusion process, such that D' varies between approximately 10^{-7} cm^2 s^{-1} (in the absence of fura-2 and of highly mobile buffer) and 4×10^{-7} cm^2 s^{-1} in the presence of fura-2 and/or highly mobile buffer.

INTRODUCTION

The concentration of free intracellular calcium $[Ca^{2+}]_i$ is determined by calcium influx, calcium release, calcium sequestration and calcium buffering. The importance of buffering is emphasized by the finding that only about 1–5% of calcium entering a cell shows up as free calcium (Hodgkin & Keynes, 1957; Smith & Zucker, 1980; Gorman & Thomas, 1980; McBurney & Neering, 1985; Ahmed & Connor, 1988); the majority is rapidly bound to cellular binding sites, and later on sequestered into calcium storing organelles or extruded by calcium transport mechanisms. In our usage, the term 'buffering' will be restricted to the rapid binding of calcium by cellular ligands, and will not include sequestration mechanisms. Neher & Augustine (1992) showed that in bovine chromaffin cells this binding is very well separable kinetically from the slow process of sequestration, which occurs on the time scale of several seconds. It can be conveniently determined by a combination of fura-2 microfluorimetry and Ca^{2+} current measurement. They showed that the 'calcium binding capacity' of cytoplasm ($d[Ca]_t/d[Ca^{2+}]_i$) has a value of approximately 75, which did not change during prolonged whole-cell recording. They concluded that the majority of cellular calcium binding sites are immobile.

Mobility of calcium buffers is a very important aspect of calcium signalling. It has become apparent recently that many calcium rises are restricted, at least for short times, to the vicinity of sites of calcium entry or release (see Augustine & Neher, 1992 for review). A mobile calcium buffer will act to disperse such domains of elevated $[Ca^{2+}]_i$ whereas fixed Ca^{2+} buffers will tend to prolong them. Correspondingly the results of previous simulations on the spatial and temporal pattern of Ca^{2+} changes following stimulation depended very much on the assumptions made about mobility of buffers (Sala & Hernandez-Cruz, 1990; Nowycky & Pinter, 1993). Thus, it is important to have experimental data on mobility of cellular Ca^{2+} buffers. The result, implicated by Neher & Augustine (1992), that there is very little mobile buffer, would mean that addition of even minute concentrations of mobile Ca^{2+} buffer, such as fura-2, during Ca^{2+} imaging experiments should alter the temporal pattern of Ca^{2+} redistribution.

Therefore, we reinvestigated the problem of mobility of Ca^{2+} buffers, focusing on the possible presence of highly mobile Ca^{2+} ligands, such as organic anions. Such buffers might have been missed in the previous investigation, since measurements were inaccurate in the first few seconds of a whole-cell recording. We did not find indications of such buffers, but found that in a fraction of cells part of the calcium binding is associated with mobile molecules in the size range of 7–20 kDa. A preliminary report of some of this work has appeared (Zhou & Neher, 1992).

METHODS

Cells and solutions

Bovine adrenal glands were obtained from a local abattoir, and chromaffin cells in primary culture were used for patch-clamp recordings 2–4 days after plating, as described previously (Fenwick, Marty & Neher, 1982*a*; see also Marty & Neher, 1985 for a modified cell culture preparation). Sizes of cells were in the range of 10–18 μm in diameter; most cells had spherical geometry, while some cells had small processes. We preferentially used relatively large spherical cells to allow better assessment of voltage-dependent whole-cell Ca^{2+} current (see below) and to get larger fluorescence signals at a fura-2 concentration of 70 μM.

To estimate the amount of Ca^{2+} influx during a depolarizing pulse by the whole-cell current, both internal and external solutions were designed to block maximally all of the voltage-dependent Na^+ and K^+ channels in chromaffin cells (Fenwick, Marty & Neher, 1982*b*; Artalejo, Mogul, Perlman & Fox, 1991). Our standard bath solution contained (mM): 125 NaCl, 5 $CaCl_2$, 2 $MgCl_2$, 2·8 KCl, 10 Hepes, 10 TEA, 0·001 TTX, pH 7·2, osmolarity 300 mosmol l^{-1}. The pipette solutions used are given in Table 1. All experiments were done at room temperature, 22 °C.

TABLE 1. Internal solutions[a]

Solution No.	Fura-2 (mM)	Nystatin (μg/ml)	Notes
1	0	0	Standard
2	0·07	250	Recording
3	0·4	0	f_{max}
4	3·0	0	Preload

[a]All internal solutions contain (mM): 145 caesium glutamate, 8 NaCl, 1 $MgCl_2$, 2 Mg-ATP, 10 Hepes, and 0·3 GTP. Differences only are noted in the table.

Combining patch-clamp and fura-2 measurement

Whole-cell (Hamill, Marty, Neher, Sakmann & Sigworth, 1981; Marty & Neher, 1983) and perforated-patch-clamp measurements (Horn & Marty, 1988) were combined with fura-2 fluorescence measurements (Grynkiewicz, Poenie & Tsien, 1985) to allow simultaneous on-line monitoring of membrane currents (I_m), two fura-2 fluorescence signals (F_1 and F_2, excited at 350 and 390 nm wavelengths respectively), and the intracellular free calcium ($[Ca^{2+}]_i$), as described earlier (Neher, 1989). In short, spatially averaged fluorescence signals were measured by a photomultiplier. They were segmented and averaged according to the state of the excitation filter wheel (revolving at 4 Hz), and held in two sample-and-hold circuits, representing the signals from the two excitation wavelengths (F_1 and F_2). The fluorescence signals, together with holding voltage and holding current were sampled and displayed at 2 Hz throughout the experiment. In all experiments the holding potential was −78 mV (corrected for liquid junction potential errors; Neher, 1992). Repetitive step depolarizations with durations of either 20 or 50 ms were applied both during nystatin-patch and whole-cell recordings to activate Ca^{2+} currents. Voltage ramps of 100 ms duration from −108 to +52 mV were applied in each experiment to determine the voltage (V_{pp}) for maximal calcium current. V_{pp} was used for the subsequent step depolarizations. Whole-cell Ca^{2+} currents were recorded at high time resolution with a computer-controlled patch-clamp amplifier (EPC-9, HEKA Electronic, Lambrecht, FRG). The 'P/4' function of the EPC-9 was used to subtract the linear leak and capacity currents (Bezanilla & Armstrong, 1977). During nystatin-patch recordings, with access resistance (R_{acc}) of 18–70 MΩ, 50% of series resistance compensation was used. Changes in fluorescence during depolarizing pulses were evaluated as described by Neher & Augustine (1992). They represent the situation after diffusional equilibration. Current integrals were evaluated using the 'Review' program (HEKA Electronic, Lambrecht, FRG). In cases where some residual Na^+ current was present (such as in Fig. 1) the integral was taken as the product of

pulse duration and plateau current. $[Ca^{2+}]_i$ was also displayed on-line according to the equation (Grynkiewicz *et al.* 1985):

$$[Ca^{2+}]_i = K_{eff}(R-R_0)/(R-R_1), \quad (1)$$

where R is the fluorescence ratio F_1/F_2, and R_0, R_1, and K_{eff} are constants which can be determined *in vivo* during whole-cell recordings using three different internal solutions: the standard internal solution (No. 1 in Table 1) to which were added (mM) either 0·1 fura-2 and 10 BAPTA (1,2-bis(*O*-aminophenoxy)ethane-*N*,*N*,*N*′,*N*′-tetracetic acid), or 0·5 fura-2 and 10 $CaCl_2$ or 0·1 fura-2, 6·6 CaBAPTA and 3·3 BAPTA (Neher, 1989). We used BAPTA as Ca^{2+} buffer for calibration solutions because it is less pH sensitive than EGTA. The dissociation constant of BAPTA was assumed to be 225 nM (the value of Tsien (1980) corrected for differences in ionic strength according to Harrison & Bers (1987)). Calibration coefficients, determined in this way on our experimental set-up were 0·073, 2·27 and 3364 nM, respectively.

For evaluation of the calcium binding capacity it is necessary to estimate the buffer capacity of the dye. Therefore the dissociation constant (K_d) of the dye has to be known. It is important to use a K_d which is consistent with the calibration constants of eqn (1). If the short wavelength of the fluorescence measurement is identical to the isosbestic point then a simple relationship exists between K_{eff} of eqn (1) and K_d (Neher & Augustine, 1992). For the more general case this can be extended to

$$K_d = K_{eff}(R_0+\alpha)/(R_1+\alpha), \quad (2)$$

where α is a coefficient which we would like to call the 'isocoefficient'. The isocoefficient can be found by searching for an α which makes the sum

$$F_i = F_1 + \alpha F_2, \quad (3)$$

independent of calcium (see Appendix E for derivation of eqn (2)). This can be done with any experimental record which shows rapid changes in calcium concentration. The signal F_i, calculated according to eqn (3), then behaves as if it were recorded at the isosbestic point. The isocoefficient is not dependent on $[Ca^{2+}]_i$, but is different for different experimental set-ups and depends on the spectral properties of fura-2. During 8 months of our experiments, α changed from 0·15 to 0·01, probably due to changes in the spectrum of the xenon UV lamp. The dissociation constant K_d of fura-2 was found to be 238 nM, as calculated by eqn (2).

Because α is sensitive to changes in the fluorescent properties of the dye, it can be used as a method to monitor dye quality. For example, in ester-preloaded cells with large amounts of Ca^{2+}-insensitive fura-2 (see Results section), α may increase above its normal value by as much as 30%.

Preparation of nystatin solution with long shelf life

Our internal solution for recording contained 250 $\mu g\ ml^{-1}$ nystatin (Sigma, USA), which makes pores in the membrane patch in the on-cell configuration (Horn & Marty, 1988). We typically reached access resistances (R_{acc} of 20–70 MΩ, which permitted voltage clamping the cell without the loss of endogenous substances by dialysis into the pipette.

Until now there have been two hindrances to using this method. First, with pipette resistances of 3–5 MΩ, one must wait 5–30 min after sealing for R_{acc} to decrease to levels low enough (30–70 MΩ) to enable reasonable voltage control (Horn & Marty, 1988; Horn & Korn, 1992). Second, the diluted nystatin (or amphotericin B) solution can be used only within 2–3 h after dilution, after which it becomes incapable of permeabilizing the plasma membrane. Thereafter nystatin solution has to be newly prepared (Horn & Marty, 1988; Rae, Cooper, Gates & Watsky, 1991; Horn & Korn, 1992). These problems have discouraged wider use of the perforated-patch method.

We have found that these two problems can be minimized by careful preparation and storage of the nystatin solution. The dilute nystatin solution is highly sensitive to light and heat (probably because of the lack of inner filter effects in dilute solution). If the dilute solution is kept in the dark and refrigerated (below or near 0 °C), the perforating activity of nystatin can be maintained for more than one week. During experiments the nystatin solution should be kept in a dark box containing ice. Even for the short time required to backfill pipettes, the nystatin solution must be protected from light exposure. Furthermore, we found that carefully dispersing nystatin solution with an ultrasonicator markedly enhances its efficacy and reduces the waiting time for permeabilization. For that the water level in the sonicator (RK100, Bandelin Electronic, Berlin,

FRG) was adjusted until the water appeared to boil (due to resonance). Then an aliquot of nystatin stock solution (5 mg nystatin in 20–50 μl dimethyl sulphoxide) was added to a small tube containing internal solution while applying the sonication. During the 2–4 min sonication the tube should be protected from light and heat.

We used Sylgard-coated patch pipettes with resistances in the range 3–5 MΩ. We dipped our pipette tips in nystatin-free internal solution for 5–15 s to fill the tips. Within 2–5 min of backfilling an on-cell gigaohm seal should be established. In most cases, within another 1–5 min R_{acc} decreased to 30–70 MΩ and voltage-clamp experiments could be performed.

The reduction in the time to reach $R_{acc} < 70$ MΩ in our experiments was probably due to the enhanced dispersion of nystatin, made possible by ultrasonicating at resonance, and partly due to appropriate choice of the tip-filling time.

Balanced loading of fura-2

Theoretically, endogenous buffer capacity, κ_S can be determined at any total intracellular fura-2 concentration ($[B]_t$) according to eqns (10) and (6) below. However, the magnitude of the error in κ_S is sensitive to $[B]_t$. It is shown in Appendix A that the lowest error of the κ_S measurement is obtained at $f = f_{max}/2$, or for $\kappa_B = \kappa_S$ (see eqn (6)). This corresponds to $[B]_t$ of about 50–100 μM for $[Ca^{2+}]_i$ of 150–750 nM.

In Neher & Augustine (1992), κ_S was estimated from fluorescence changes in response to several depolarizing pulses applied at different $[B]_t$ levels during loading of fura-2. In this study we preloaded cells with fura-2 to about 70 μM, and used the same fura-2 concentration in the nystatin and whole-cell recording pipette. Thus, there was only little or no change in $[B]_t$ during whole-cell dialysis which minimized errors in our κ_S estimate. This was very important because the mobility of endogenous Ca^{2+} buffers was assessed by evaluating κ_S changes during the transition from nystatin-perforated-patch to whole-cell recording (see Results).

We preloaded cells in two different ways. The first approach was standard fura-2 ester loading (Grynkiewicz *et al.* 1985) with 5–10 min incubation at 37 °C and 1·5 μM fura-2 ester followed by at least 30 min of incubation in standard bath solution. The second one was by means of a short 'whole-cell' episode with a pipette containing high fura-2 salt concentration (3 mM). To minimize the loss of mobile endogenous Ca^{2+} buffers, the loading time was made very short (2–5 s), during which levels of ~ 70 μM were reached. We stopped loading by simply pulling the pipette away from the cell. Based on Pusch & Neher (1988), one can estimate that less than 10% of buffers of molecule mass more than 100 Da will escape with this method. This whole-cell preloading method was preferred because very often there were Ca^{2+}-insensitive forms of fura-2 in the ester-loaded cells (see Results section), which introduced serious errors.

Theory for endogenous Ca^{2+} buffer measurements

Neher & Augustine (1992) have developed a method for measuring endogenous Ca^{2+} buffers which will be used in this paper. Briefly, the intracellular exogenous fura-2 and endogenous Ca^{2+} buffers compete for Ca^{2+} binding after Ca^{2+} influx. For times short with respect to the time constant of Ca^{2+} retrieval and Ca^{2+} pumping, conservation of total calcium requires

$$\Delta[Ca^{2+}]_i + \Delta[BCa] + \Delta[SCa] = \Delta[Ca]_t, \quad (4)$$

where Δ represents a change in a particular value, B represents fura-2, and S represents other Ca^{2+} buffers, including endogenous buffers and exogenous buffers other than fura-2. [BCa] and [SCa] are concentrations of Ca^{2+} bound by B and by S, respectively. $[Ca]_t$ is the total concentration of calcium including free and bound forms. In practice, $\Delta[Ca]_t$ represents Ca^{2+} influx which can be elicited and measured by the whole-cell voltage-clamp technique, while $[Ca^{2+}]_i$ and [BCa] can be obtained by the fura-2 technique. According to the theory of Neher & Augustine (1992) the Ca^{2+} binding capacity of cytoplasm, κ_S, defined as

$$\kappa_S = d[SCa]/d[Ca^{2+}]_i, \quad (5)$$

can be calculated from the experimental quantity, f, by:

$$\kappa_S = \kappa_B(f_{max}/f - 1) - 1, \quad (6)$$

where f is the ratio of fluorescence change over Ca^{2+} current integral during a short pulse of Ca^{2+} influx:

$$f = \Delta F_2 / \int I_{Ca}\, dt. \quad (7)$$

The value, f_{max}, is the maximum value of f observed in the case of fura-2 being the dominating buffer and κ_B is the Ca^{2+} binding capacity of fura-2. κ_B is defined in analogy to κ_S:

$$\kappa_B = d[BCa]/d[Ca^{2+}]_i, \tag{8}$$

and, at fixed total intracellular concentration of fura-2 $[B]_t$, is given by

$$\kappa_B = \frac{[B]_t/K_d}{(1+[Ca^{2+}]_i/K_d)^2}, \tag{9}$$

where K_d is the dissociation constant of fura-2.

In the case of appreciable changes in $[Ca^{2+}]_i$ during voltage pulses κ_B should be replaced by a 'mean binding capacity', κ'_B:

$$\kappa'_B = \frac{[B]_t/K_d}{(1+[Ca^{2+}]_a/K_d)(1+[Ca^{2+}]_b/K_d)}, \tag{10}$$

where $[Ca^{2+}]_b$ and $[Ca^{2+}]_a$ are $[Ca^{2+}]_i$ immediately before and after a depolarization-induced Ca^{2+} influx. In chromaffin cells 0·4 mM fura-2 was found to be enough to bind all calcium entering during moderate pulses (20–50 ms duration; Neher & Augustine, 1992). Therefore the value of f measured in a cell loaded with 0·4 mM fura-2 can be used for f_{max}.

In the whole-cell configuration $[B]_t$ in eqn (10) can be determined by

$$[B]_t = [B]_p F_i/F_{i\infty}, \tag{11}$$

where $[B]_p$ is the fura-2 concentration of the pipette. F_i is the fluorescence signal as calculated according to eqn (3) at a given time and $F_{i\infty}$ is the same after diffusional equilibrium between pipette and cytoplasm has been reached during standard whole-cell recording.

For a given experimental set-up the quantity f_{max}, reflecting the relative sensitivities of the fluorescence measurement and the current measurement, should be constant. To eliminate long-term drifts in fluorescence sensitivity we evaluated the fluorescence of a standard (Fluoresbrite BB-beads, article No. 18340, Polyscience, Inc, Warrington, PA, USA) at the end of each day's experiments and related all fluorescence values (before entering into eqn (7)) to the fluorescence intensity of the beads (Neher & Augustine, 1992).

Experiments to determine f_{max} were done using solution No. 3 in Table 1, according to Neher & Augustine (1992). Since f_{max} is dependent on dye properties and on the set-up, we repeated f_{max} experiments whenever a new lot of fura-2 was used, or if there were significant changes in the fluorescent beads' signals.

Equation (6) provides a way to estimate κ_S from a single depolarizing pulse, provided that one knows f_{max}, which is determined by a separate experiment with high fura-2 concentration. In Appendix D, we describe another method for κ_S measurement. The latter method does not require knowledge of f_{max}, but it uses fluorescence and I_{Ca} data from two depolarizing pulses of different magnitude. It rests on the assumption (borne out by experiments) that κ_S is independent of $[Ca^{2+}]_i$. The method using eqn (6) is preferred for tracking the time course of calcium buffering and is used for all κ_S values reported here.

Measurement of Ca^{2+} binding capacity of pipette-filling solutions

To measure the Ca^{2+} binding capacity of our internal solution, we used a chamber containing 2 ml of standard internal solution to which we added 25 μM mag-fura-2, a fluorescent Ca^{2+} indicator with an excitation–emission spectrum similar to that of fura-2. The dissociation constant of mag-fura-2 is 44 μM, which allows calcium measurements in the range 5–100 μM (Baylor, Hollingworth & Konishi, 1989). Defined amounts of Ca^{2+} were added to the chamber and increases in free Ca^{2+} concentration, $\Delta[Ca^{2+}]_i$, were recorded. The Ca^{2+} binding capacity of the pipette-filling solution, was then calculated by analogy to eqn (8).

Detecting and compensating for intracellular Ca^{2+}-insensitive fura-2

Ca^{2+}-insensitive fura-2 was found in leukocytes loaded with the acetoxymethyl ester of fura-2, fura-2 AM (Scanlon *et al.* 1987). A small amount of intracellular Ca^{2+}-insensitive fura-2 can result in a serious underestimate of $[Ca^{2+}]_i$ and an overestimate of κ_B and κ_S. Thus, it is necessary to assess how much Ca^{2+}-insensitive fura-2 is present in every cell which has been preloaded by fura-2 AM, and then to subtract its contribution from the F_1 and F_2 signals.

Let r be the fraction of Ca^{2+}-insensitive fura-2 fluorescence, defined as the ratio,

$$r = F_{ib}/F_i, \tag{12}$$

where F_{ib} is the contribution of the 'background' to F_i (for F_i see eqn. (3)). The background may include fluorescence from non-hydrolysed fura-2 ester, from compartmentalized fura-2 which does not respond to cytoplasmic Ca^{2+} changes, and also from cell autofluorescence. For any wavelength we have

$$F_x = F_{xe} + F_{xb}, \tag{13}$$

where the subscript x stands for wavelength (1, 2 or i for quasi-isosbestic). Here, and in the following, subscripts e and b stand for corrected and background parts respectively. Also we use primed symbols (e.g. R') to designate the unprimed symbols and incremented by α, such as $R' = R + d = (F_1 + \alpha F_2)/F_2 = F_i/F_2$,

$$R'_b = R_b + \alpha = F_{ib}/F_{2b}. \tag{14}$$

Then, we have

$$R'_e = (F_i - F_{ib})/(F_2 - F_{2b}) = R'(1-r)/(1 - rR'/R'_b), \tag{15}$$

$$R_e = (1-r)/(1/R' - r/R'_b) - \alpha, \tag{16}$$

where R_e is the corrected fluorescence ratio, which can be entered into eqn (1) instead of R to yield corrected $[Ca^{2+}]_i$.

With the same definitions and eqn (11) we have

$$[B]_{te} = [B]_p(F_i - F_{ib})/(F_{i\infty} - F_{ib\infty}), \tag{17}$$

where F_{ib} and $F_{ib\infty}$ are the background components of signals F_i and $F_{i\infty}$, as used in eqn (11). This, together with eqns (12)–(14) yields

$$[B]_{te} = \frac{[B]_p(1-r)F_i}{(1-r_\infty)F_{i\infty}}, \tag{18}$$

where r_∞ is r after whole-cell diffusion equilibrium.

We have used three ways to obtain the parameter r, which characterizes background fluorescence. The simplest and most direct way is to destroy the plasma membrane at the end of an experiment; the fluorescence signals from the cell remains are taken as F_{xb}, and r and R_b are calculated from eqns (12) and (14). We designate r calculated this way as 'r_1'. It is a lower-limit estimate of r since r_1 includes only the immobile part of F_{xb}.

The second way to estimate r, which will be designated as 'r_2', is based on the difference between the calibration parameter R_1 and the fluorescence ratio R_s measured with a large depolarization-induced Ca^{2+} influx. This method rests on the assumption that the Ca^{2+} influx saturates the intracellular fura-2 and that therefore a difference between R_1 and R_s is solely due to background fluorescence. We have (see Appendix B),

$$r_2 = \left(1 - \frac{R_1 + \alpha}{R_s + \alpha}\right) \Big/ \left(1 - \frac{R_1 + \alpha}{R_b + \alpha}\right). \tag{19}$$

R_b has to be known in this method, and we usually assume that it is the same as that found by the r_1 method. The value r_2 is an upper estimate of r, because $[Ca^{2+}]_i$-dependent inactivation of Ca^{2+} channels (Eckert & Chad, 1984) may prevent $[Ca^{2+}]_i$ from reaching high enough levels; r_2 can be determined both during nystatin and whole-cell recording.

The third way of estimating r rests on the finding (Neher & Augustine, 1992) that the calcium binding capacity, κ_S, is independent of $[Ca^{2+}]_i$ in the range up to 2 μM. With the assumption that deviations from that rule are due to background fluorescence, an estimate for 'r_3' can be obtained by comparing the responses to two stimuli of different strengths. In the derivation of an equation for r_3 (Appendix C) the simplifying assumption has to be made that the weak stimulus provides an accurate estimate of κ_S. This is justified by the fact that at low $[Ca^{2+}]_i$ errors caused by background fluorescence are quite small, due to a large fura-2 signal at wavelength 2 (390 nm). During this measurement the weak stimulus should not elevate $[Ca^{2+}]_i$ to values more than 450 nM, whereas the strong stimulus should increase $[Ca^{2+}]_i$ to between 750 nM and 1·5 μM. This method, which also

requires prior knowledge of R_b, does not perturb cells as much as the other two methods. We found it is very important to routinely evaluate the quantity r, mostly in the form of r_3, not so much as a quantitative assay of background fluorescence, but rather as a means to check for its presence and for internal consistency of the measurements.

RESULTS

Figure 1 shows a typical 'balanced-loading' experiment, in which the fura-2 content of the pipette almost matched that of a 'preloaded' cell. Figure 1*B* is the whole-cell current response to a voltage ramp, applied during the nystatin-patch episode of that experiment. The absence of outward current suggests that all of the voltage-dependent K^+ current was blocked. V_{pp}, the potential of peak Ca^{2+} current, was 17 mV. Figure 1*C* shows the current response to a 20 ms step depolarization from a holding potential of −78 to +17 mV. In the absence of voltage-dependent Na^+ and K^+ currents, all of the current should be I_{Ca}, and the area between the zero line and downward current trace should represent the total influx of Ca^{2+}. In this cell, however, there was some residual fast-inactivating (time constant, 2–3 ms) Na^+ current in spite of the presence of 1 μM TTX.

Figure 1*A* shows a time-compressed print-out of fluorescence and current traces of the whole experiment including nystatin and whole-cell recording episodes. The large arrow indicates the time at which the nystatin patch was ruptured by a short suction pulse applied to the pipette (Hamill *et al.* 1981), leading to the whole-cell configuration. R_{acc} decreased from 30 to 10 MΩ during this transition. After obtaining the whole-cell configuration there was a small increase of the F_i signal, suggesting some net fura-2 diffusion from the pipette into the cell. The slight increase in the basal level of $[Ca^{2+}]_i$ upon initiating whole-cell recording is quite typical in our balanced-loading experiments, perhaps due to the rather poorly Ca^{2+}-buffered internal solutions. During up to 2000 s of whole-cell recording, most cells shifted the voltage V_{pp} of peak I_{Ca} by 5–10 mV to a more negative direction as described by Marty & Neher (1983). With standard internal solutions, the typical peak I_{Ca} of a 14 μm cell was about 600 pA during perforated recording, and decreased 20–50% during more than 1000 s whole-cell dialysis. Membrane resistance during whole-cell recording was similar to that prior to rupture of the nystatin patch (3–8 GΩ, see Fig. 1) even during more than 1000 s of recording.

During both nystatin-patch and whole-cell recording, repetitive depolarizing pulses were applied under voltage-clamp control. The resulting Ca^{2+} influxes through voltage-dependent Ca^{2+} channels were accompanied by step-like decreases in the Ca^{2+}-sensitive fluorescence at 390 nm excitation wavelength and by step-like increases in $[Ca^{2+}]_i$. All of these signals are required to calculate κ_S, the capacity of endogenous Ca^{2+} buffers.

Autofluorescence of cells and other forms of background fluorescence disturb estimation of $[Ca^{2+}]_i$, as discussed in the Methods section. The level of autofluorescence in our chromaffin cells increased with time after cell plating, typically doubling from day 1 to day 3. The fluorescence ratio of autofluorescence was approximately 0·2, which is similar to that of fura-2 fluorescence at 150 nM $[Ca^{2+}]_i$. The fluorescence intensity was typically 2–5% of that of a cell loaded with 70 μM fura-2. Unloading experiments showed that about 50% of autofluorescence washed out during whole-cell experiments ($n = 5$). To minimize the interference of auto-

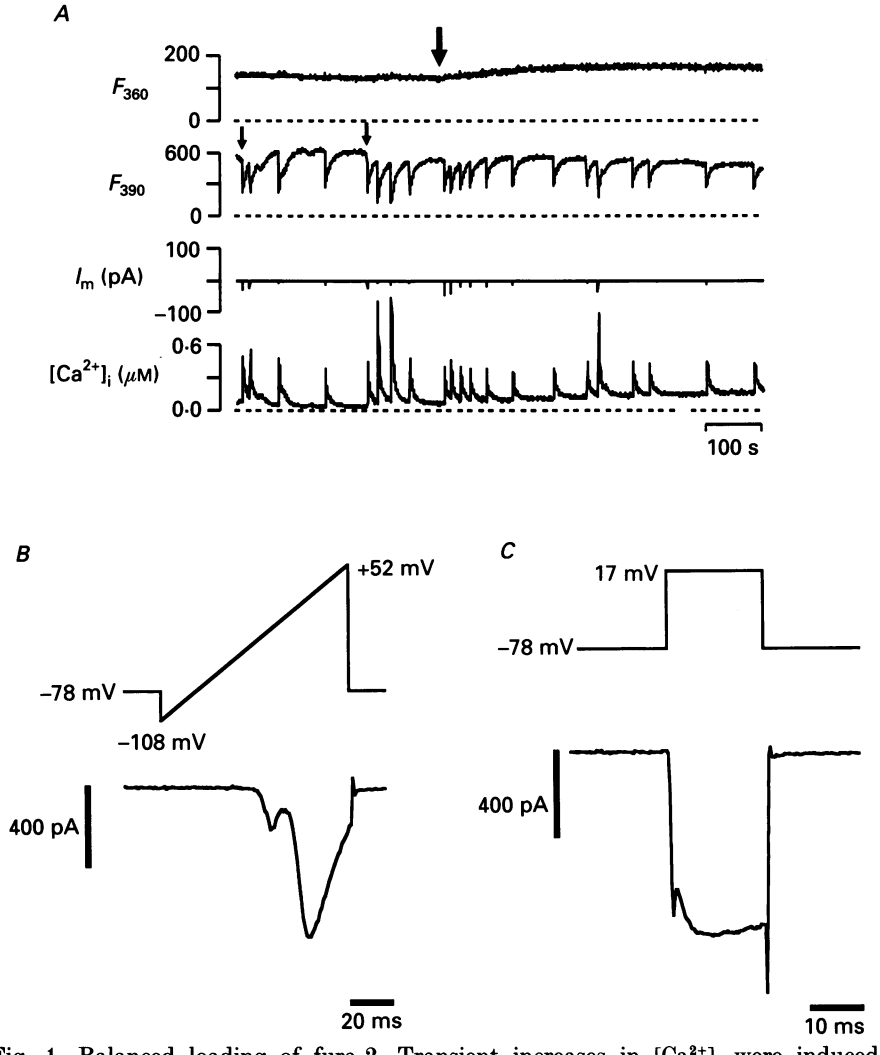

Fig. 1. Balanced loading of fura-2. Transient increases in $[Ca^{2+}]_i$ were induced by depolarizing pulses during nystatin-patch and whole-cell recording. *A* shows the whole experiment at compressed time scale. Traces from top to bottom are fluorescence ($F_{360} = F_1$) according to eqn (3), fluorescence excited at 390 nm ($F_{390} = F_2$), whole-cell current (I_m), and $[Ca^{2+}]_i$ respectively. We show the current trace to document that there were no leaks or major changes in holding current throughout the experiment. The deflections during voltage pulses are not resolved and should only be taken as time markers for the stimuli. Ten minutes before this recording the cell was preloaded with fura-2 by attaining the whole-cell configuration for 3 s with a 'loading' pipette containing 3 mM fura-2. The loading pipette was removed, and the cell was allowed to recover before a second pipette (containing the nystatin solution) was applied to the cell. The first and second small arrows indicate the times at which *B* and *C* were recorded, respectively. The large arrow indicates the time at which a short pulse of suction was applied to the pipette to rupture the patch, before and after which the cell was in nystatin-patch and whole-cell configuration, respectively. *B*, inward currents evoked by a 100 ms ramp (−108 to −52 mV) from a holding potential of −78 mV. Peak I_{Ca} in this cell occurred at 17 mV. The small peak at −14 mV is sodium current which is incompletely blocked by 1 μM TTX. *C*, I_{Ca} evoked by a 20 ms depolarization to +17 mV.

fluorescence we routinely subtracted out averaged autofluorescence from the baseline. This should reduce the errors in κ_S due to autofluorescence to less than 5% in all our experiments.

κ_S *estimated in cells preloaded by fura-2 AM*

Figure 2 shows an experiment in which a cell was preloaded with fura-2 AM. With some experience we managed to adjust the loading conditions such that we achieved

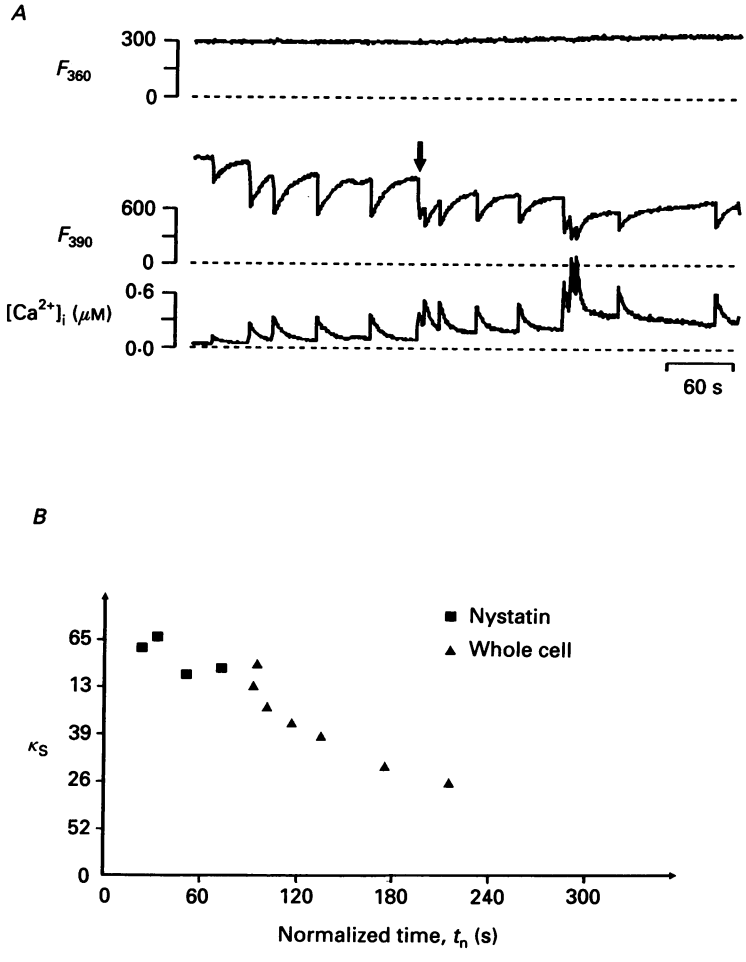

Fig. 2. Balanced-loading experiment with the cell preloaded with fura-2 AM. *A*, original fluorescence records. The arrow indicates the time when the nystatin patch was ruptured by a pulse of suction. *B*, κ_S calculated during nystatin-patch and whole-cell recording was plotted against recording time, to determine the wash-out of the buffer capacity. Note that time in *B* is normalized: $t_n = 10^4 \times t/(R_{acc}\, d^3)$, with recording time, t, in seconds, cell diameter, d, in micrometres and access resistance, R_{acc}, in megaohms. This normalization eliminates scatter when comparing cells of different diameter and access resistance (Pusch & Neher, 1988). The normalization is unity for a cell with 10 μm diameter and 10 MΩ access resistance. One hundred seconds of normalized time correspond to 220 s in real time in this experiment.

'balanced loading' also with this method. Initially the cell was in the perforated-patch configuration. At the arrow the patch was ruptured by suction to begin whole-cell recording. In Fig. 2*B* κ_S is plotted against time, to track wash-out of endogenous buffer. During perforated-patch recording, κ_S was about 52 ± 7, while following

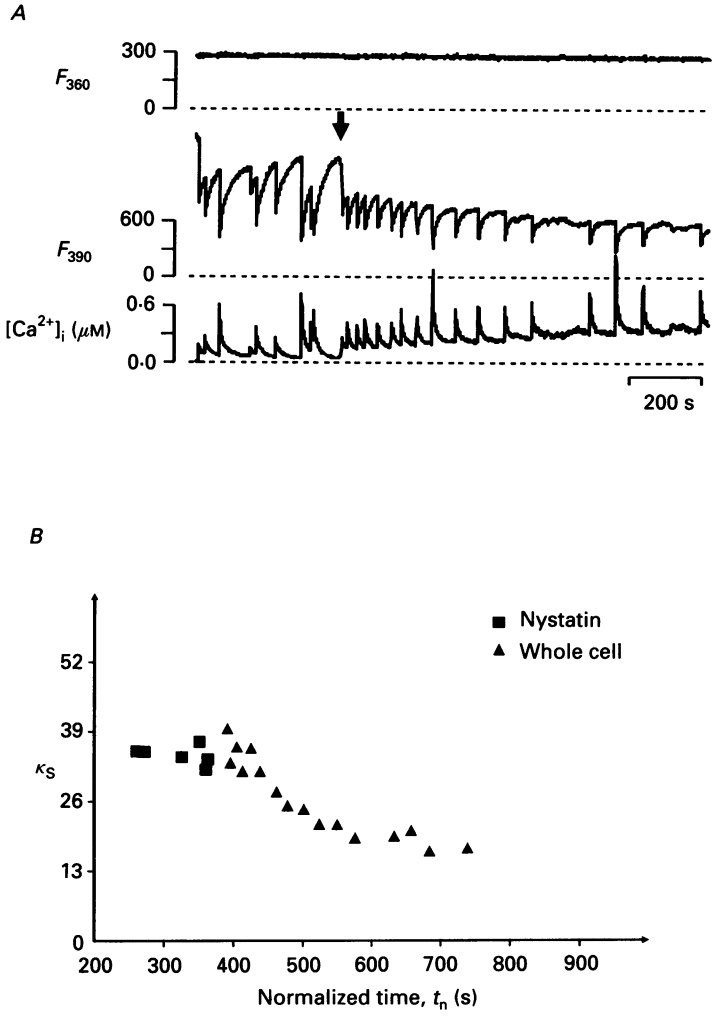

Fig. 3. Example of a chromaffin cell with a large mobile fraction of endogenous Ca^{2+} buffers, detected by a 'double whole-cell' experiment. The cell was preloaded by a short (3 s) whole-cell episode 10 min prior to the illustrated recordings. *A*, fluorescence traces. The arrow indicates the time of patch rupture. *B*, time course of κ_S. During whole-cell dialysis κ_S decreased monoexponentially to 50% of its initial value, suggesting that some of the endogenous Ca^{2+} buffers were mobile in this particular cell.

initiation of whole-cell recording κ_S decreased to about 50% of the initial level over 150 s (normalized time, see legends in Fig. 2). In this cell, 10% of the total fura-2 was Ca^{2+} insensitive ($r_3 = 10\%$) as estimated by eqn (A 18) assuming $R_b = 0{\cdot}25$. κ_S was calculated applying the correction for background fluorescence, given by eqns (16) and (18).

In eight ester-preloaded cells with $r_3 \leqslant 15\%$ and with no detectable mobile Ca^{2+}-insensitive fura-2 (see below), the mobile endogenous buffer ranged between 0 and 50% of the total buffer with an average value of 25%. The average κ_S in these cells was 45 before onset of whole-cell recording.

κ_S *estimated in cells preloaded by a short whole-cell episode*

Ca^{2+}-insensitive fura-2 in fura-2 AM-loaded cells introduces a potential source of error in the calculation of κ_S. This is particularly severe if part of the Ca^{2+}-insensitive

TABLE 2. Data for calculating Fig. 3*B*[a]

t_n (s)	$[Ca^{2+}]_i$ (nM)	κ_B	ΔF_2	Ca^{2+} charge (pC)	f_{max}/f	κ_S	Recording method
257	318	57·3	414	13·3	1·62	34·8	NP[b]
271	737	28·6	729	32·4	2·25	34·7	NP
325	276	71·5	553	16·2	1·49	33·7	NP
350	830	27·9	893	41·5	2·35	36·5	NP
360	512	34·1	453	17·5	1·95	31·4	NP
362	771	18·0	296	17·0	2·90	33·3	NP
390	301	62·4	452	14·7	1·64	39·0	WC[c]
395	531	30·7	345	14·3	2·10	32·7	WC
404	477	35·0	356	14·4	2·05	35·6	WC
412	565	28·5	337	14·2	2·13	31·2	WC
425	515	31·4	333	14·2	2·16	35·4	WC
438	544	28·9	337	14·0	2·11	31·1	WC
462	611	25·3	341	14·3	2·12	27·3	WC
478	1442	9·83	463	33·2	3·63	24·8	WC
501	768	17·9	298	14·1	2·40	24·1	WC
523	803	17·4	322	14·5	2·28	21·4	WC
549	827	16·5	297	13·8	2·35	21·3	WC
575	911	14·3	288	13·6	2·39	18·8	WC
631	1118	10·3	249	14·5	2·95	19·1	WC
683	1245	9·12	238	13·7	2·91	16·4	WC
738	1170	9·59	227	12·9	2·87	16·9	WC

[a] The intracellular fura-2 concentration was constant at 70 μM throughout this recording (see trace F_{360} in Fig. 3*A*).
[b] NP refers to nystatin-patch recording.
[c] WC refers to whole-cell recording. t_n, normalized time (see legend of Fig. 2); for definition of other symbols see eqns (5)–(9) in Methods section.

fura-2 is mobile, which makes the compensation of the background effect more difficult (see below). To avoid this problem, we used cells preloaded by 2–5 s of whole-cell dialysis with a 'loading' pipette. The fura-2 salt used in the loading pipette and that used in the whole-cell recording pipette (for balanced loading) were from the same stock of fura-2 solution, differing only in its final concentrations: 3 mM in the first and 70 μM in the second pipette.

Figure 3 shows such a double whole-cell experiment. The cell was preloaded by a short (4 s) whole-cell episode (not shown) with 3 mM fura-2 in the pipette (solution No. 4 in Table 1). A perforated-patch recording was established on the same cell, which reached $R_{acc} = 40$ MΩ about 10 min after the preloading. The second pipette contained 70 μM fura-2 and nystatin (solution No. 2 in Table 1). One 100 ms ramp (−108 to +52 mV), followed by 20 or 50 ms step depolarizations was applied. The

large arrow indicates patch rupture, at which time R_{acc} decreased from 27 to 6 MΩ. The absence of any change in F_i during whole-cell dialysis suggests that the preloaded intracellular fura-2 concentration was close to 70 μM. To rule out artifacts in κ_S determination from possible systematic errors in our $[Ca^{2+}]_i$ measurement, two

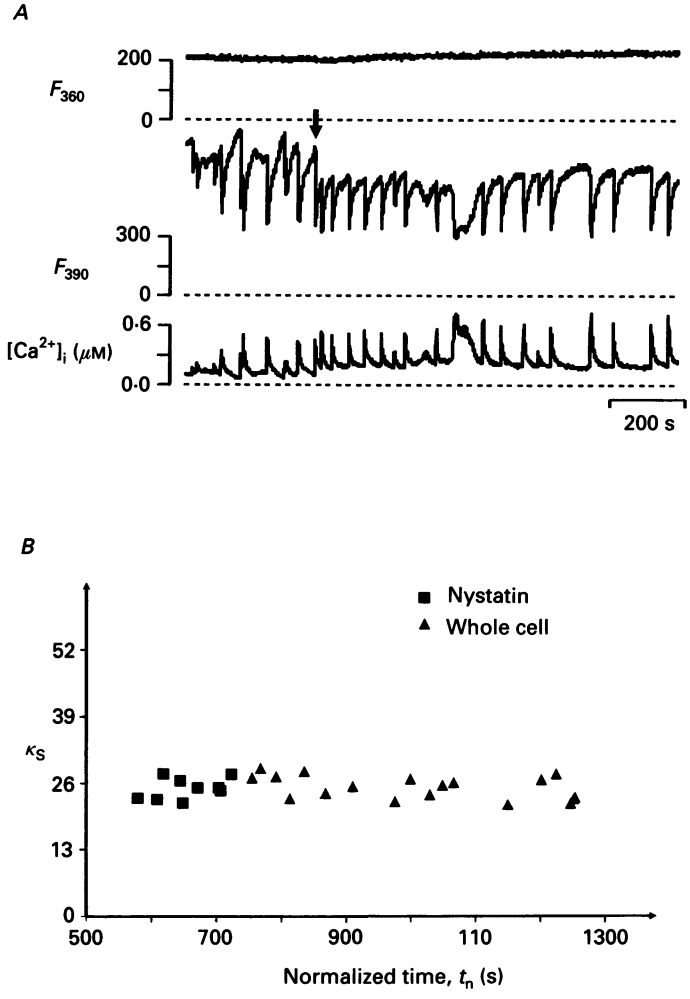

Fig. 4. Example of a cell with only a minor fraction of mobile endogenous Ca^{2+} buffers, assessed by a 'double whole-cell' experiment as in Fig. 3. *A*, fluorescence traces. *B*, time course of κ_S. In contrast to the case illustrated in Fig. 3, here κ_S remained constant during whole-cell dialysis, suggesting that all of the endogenous Ca^{2+} buffers are immobile.

precautions were undertaken: first, 20 ms was the standard duration for most depolarizing stimuli; second, pulses were not applied until the $[Ca^{2+}]_i$ returned to near-resting levels. These precautions ensured that most of the parameters required to calculate κ_S using eqns (6)–(11), were constant, such that any changes obtained following patch rupture could safely be attributed to true changes in κ_S. Calculations of κ_S for several stimuli from this experiment are shown in Table 2 and are plotted as a function of time in Fig. 3*B*. During whole-cell dialysis, κ_S decreased exponentially

from 36 to about 18 with a time constant of 100 s, suggesting that 50% of the endogenous Ca^{2+} buffer in this cell diffused into the pipette.

The amount of mobile Ca^{2+} buffer differs from cell to cell. Figure 4 shows another experiment similar to that of Fig. 3, but with little κ_S decay during whole-cell dialysis. The mobile buffer in this cell comprises less than 10% of the total κ_S.

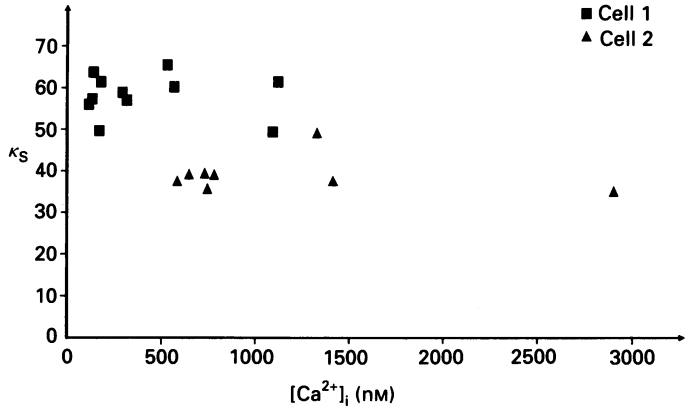

Fig. 5. $[Ca^{2+}]_i$ independence of endogenous Ca^{2+} buffers. Cell 1 was recorded in nystatin-patch configuration (see text). Cell 2 was recorded after 500 s of whole-cell dialysis. Depolarizing pulses with durations 20, 50, 100 and 200 ms were applied to load the cell to different $[Ca^{2+}]_i$ levels.

In twenty-five double whole-cell experiments, total mobile buffers ranged from 0 to 50% of total endogenous buffer with a mean value of 20%. While variation in the amount of mobile buffer is large, the normalized time constant (see legend to Fig. 2) of κ_S wash-out is quite constant at 95 ± 5 s, suggesting that the detected buffers have a similar molecular weight. The (normalized) wash-out time constant of fura-2 is 35 ± 3 s (mean $\pm$ S.E.M., $n = 10$).

Comparing the time constant of mobile buffer with that of fura-2 allows a prediction of the molecular weight of the diffusing substance. With a molecular mass for fura-2 of 637 Da, and a third-power relationship between molecular mass and diffusion time constant (Pusch & Neher, 1988) one arrives at an estimate of 13 ± 6 kDa for the mobile buffer molecules.

The affinity of Ca^{2+} buffers

The affinity of the buffers for calcium is quite low. Figure 5 shows the $[Ca^{2+}]_i$ dependence of κ_S for two cells. Cell 1 was measured during a nystatin-patch recording. The data from cell 2 were measured after 400 s (normalized time) of whole-cell dialysis, such that all mobile buffers have been washed out. The $[Ca^{2+}]_i$ given in the figure is the average of that before and after each pulse. The data illustrated were generated by pulses with durations of 20, 50, 100 and 200 ms respectively. κ_S remained constant in both cases while the $[Ca^{2+}]_i$ changed from 100 to 1200 nM (see also Table 2). According to eqn (10), if the dissociation constants of the buffers were

smaller than 2·5 μM, κ_S at $[Ca^{2+}]_i$ = 1200 nM should be 50% smaller than that at 100 nM (cell 1 was found to contain 50% of mobile buffer in the whole-cell recording following the experiment of Fig. 5). Since no decrease in κ_S with increasing $[Ca^{2+}]_i$ was found in ten similar experiments it is suggested that both mobile and immobile endogenous Ca^{2+} buffers have dissociation constants > 2 μM. Constancy of κ_S was always observed, where tests for background fluorescence were negative (see below).

The presence of intracellular Ca^{2+}-insensitive fura-2

In cells preloaded with fura-2 AM, Ca^{2+}-insensitive fluorescence background was found to be present, as determined by three different methods. These measurements are based on residual fluorescence after unloading (r_1), fluorescence during a saturating Ca^{2+} signal (r_2), and comparison between κ_S values at widely different $[Ca^{2+}]_i$ (r_3), respectively (see Methods). In ten experiments we combined two or even three of these. The agreement between r_2 and r_3 is quite good. As expected $r_1 \leqslant r_2$ or r_3, since r_1 includes only the immobile part of Ca^{2+}-insensitive fura-2. The parameter R_b (eqn (14)) can only be obtained through the measurement of r_1. The value found corresponds to a $[Ca^{2+}]_i$ between 15 and 150 nM ($n = 5$), which is similar to the basal level of the cell. We assume this value to hold for all our measurements, although it may be different, since different contributions to background fluorescence may have different spectral properties. In about 20% of cells there was no or only a small background fluorescence (r_2 and/or $r_3 < 0{\cdot}05$), comparable to autofluorescence. In about 20% of cells there was evidence for mobile Ca^{2+}-insensitive fura-2, as determined by comparing r_2 measured both during nystatin-patch and during whole-cell recording. In some cases κ_S calculated from uncorrected fluorescence data decayed during whole-cell recording with a normalized time constant of 35 s, the same as that of fura-2 wash-out. This was also taken as evidence for mobile background fluorescence. In a few cells, more than 50% of the fura-2 was Ca^{2+} insensitive. Figure 6 is an extreme example of such a cell. This cell had average size (11 μm) and average voltage-dependent I_{Ca} (250 pA). Large depolarizing pulses (1000 ms in duration) were applied both during nystatin-patch and during whole-cell recording, as indicated by an asterisk in Fig. 6*A*, to saturate the intracellular fura-2. While the total fura-2 concentration (represented by the F_i signal) during the nystatin-patch recording was larger than that in whole-cell, the response of Ca^{2+}-sensitive fluorescence (F_2) at the asterisk was much smaller in the nystatin-patch than that in whole-cell. This can be explained by the presence of intracellular Ca^{2+}-insensitive fura-2, which is replaced by Ca^{2+}-sensitive fura-2 from the pipette during whole-cell dialysis. In fact the compartment ratio, r_2, as determined by eqn (19) is 75% during nystatin-patch recording and 18% during whole-cell recording. Figure 6*B* shows the time course of κ_S, calculated by eqn (6), without compensation for background fluorescence in order to emphasize the artifact that Ca^{2+}-insensitive fura-2 can cause. Due to the large amount of Ca^{2+}-insensitive fura-2 during the nystatin-patch recording, $[Ca^{2+}]_i$ was severely underestimated, and κ_B and κ_S were much overestimated. While Ca^{2+}-sensitive fura-2 diffuses into the cell and Ca^{2+}-insensitive fura-2 diffuses out of the cell, κ_S becomes smaller and smaller. The decay has a normalized time constant of 35 s, which is the same as the wash-out time constant of fura-2.

These experiments ($n = 4$) provide direct evidence that in some of the chromaffin cells preloaded by fura-2 AM there is a portion of fura-2 which is Ca^{2+} insensitive and that part of this Ca^{2+}-insensitive fura-2 is mobile.

Large amounts of mobile Ca^{2+}-insensitive fura-2 also altered the isocoefficient α in eqn (3). During whole-cell dialysis in Fig. 6, α changed from 0·15 to 0·10.

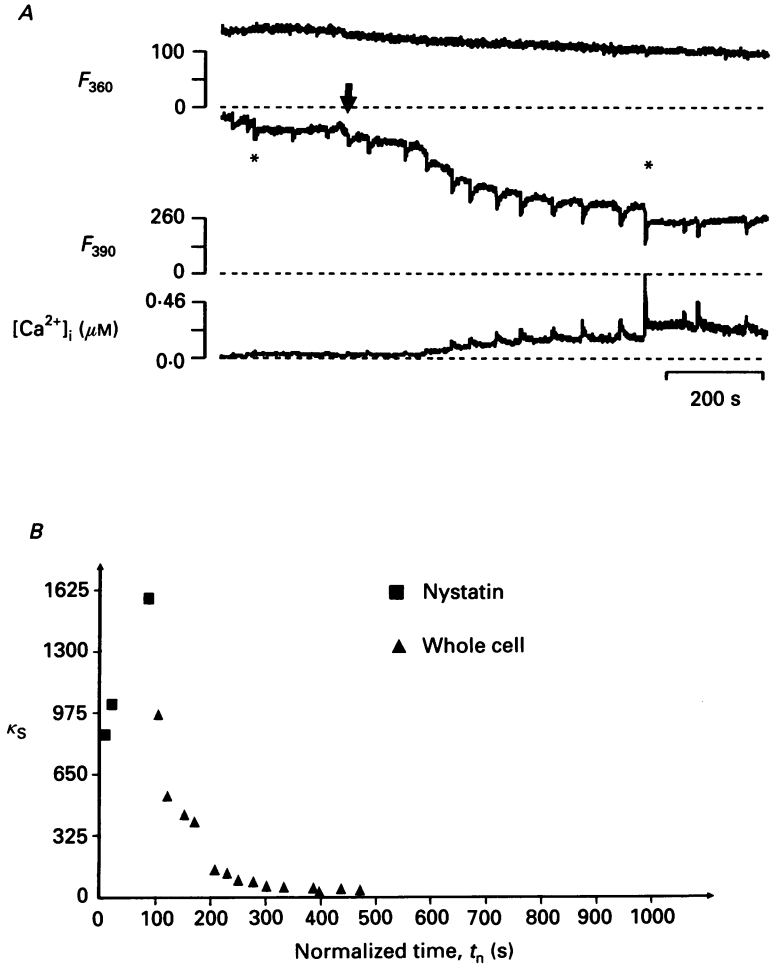

Fig. 6. Evidence for a fura-2-derived mobile Ca^{2+}-insensitive fluorophore in a cell loaded by the ester method. The cell was incubated in 1·5 μM fura-2 AM for 5 min at 37 °C, 1 h before the experiment. *A*, fluorescence recording. The cell had normal voltage-dependent Ca^{2+} currents (250 pA). Depolarizing pulses of 1 s duration were applied (indicated by the asterisks) both during nystatin-patch and whole-cell recording. Such long pulses saturate fura-2. Although Ca^{2+}-insensitive fluorescence, $F_i(F_{360})$, was larger during the nystatin-patch recording than after obtaining whole-cell configuration, the Ca^{2+}-induced decrement at 390 nm was much smaller (see text). *B*, large κ_S artifact from Ca^{2+} insensitive fura-2. κ_S was calculated from eqn (6). Because $[Ca^{2+}]_i$ was underestimated due to the presence of the Ca^{2+}-insensitive fura-2, κ_B and κ_S were overestimated. Note that the time constant of κ_S decay is the same as that of fura-2 (35 s), indicating wash-out of a fura-2-like substance.

Permeability of nystatin pores to small Ca^{2+} binding anions

In the experiments described so far we compared κ_S between nystatin-permeabilized patch and whole-cell recordings and concluded that there was no detectable wash-out of highly mobile endogenous Ca^{2+} buffer after rupture of the

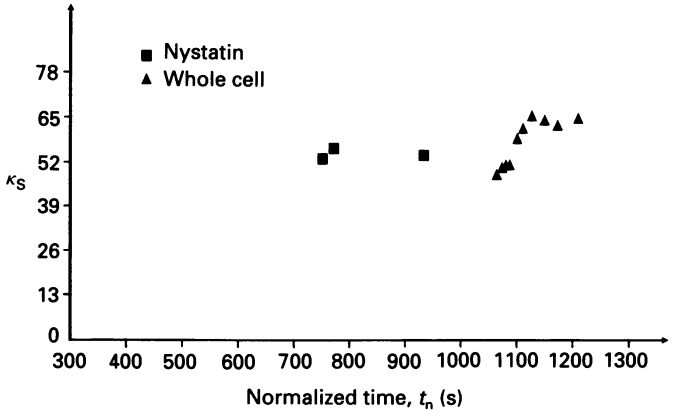

Fig. 7. 'Wash-in' of exogenous Ca^{2+} buffers. The cell was preloaded by a short whole-cell episode (with solution No. 1 of Table 1). The recording pipette contained solution No. 2 of Table 1 with the addition of 10 mM diglycolic acid (pH 7·2, osmolarity 310 mosmol l^{-1}). During more than 700 s nystatin recording the access resistance, R_{acc}, was less than 32 MΩ. Then the membrane patch was ruptured, and depolarizing pulses were applied to follow the wash-in of the Ca^{2+}-binding diglycolic acid (DA) anions. κ_S increased about 25% within 70 s of attaining the whole-cell configuration. Then κ_S stopped increasing, suggesting equilibration of DA between the pipette and cytoplasm.

patch. As candidates for highly mobile buffers we expect organic anions and metabolites such as maleate, isethionate, nucleotides and perhaps phosphocreatine. These substances with molecular masses of several hundred daltons would be expected to wash out within about 10 s. However, if the nystatin pores were permeable to some of these anions, they could escape from the cell before whole-cell recording. We did not observe any systematic downward trend of κ_S during nystatin recording, which suggests that such 'wash-out' does not occur. Furthermore we performed experiments to observe 'wash-in' of Ca^{2+} binding capacity contained in the patch pipette. Our normal caesium glutamate-based internal solution (No. 1 in Table 1) has very little Ca^{2+} binding capacity (κ). We measured it, as described in Methods, and found a value of 3. In order to increase κ we added 10 mM diglycolic acid (DA, caesium salt) to solution No. 1 (Table 1). We chose diglycolate, a divalent anion, because we could not find a monovalent organic anion with high enough Ca^{2+} affinity. The resulting solution had a Ca^{2+} binding capacity of 20 (measured *in vitro*, pH 7·2). Such high Ca^{2+} binding capacities should be detectable as 'wash-in' after rupturing the nystatin patch, if the nystatin pores were not permeable to DA. Figure 7 shows such a double whole-cell experiment. The nystatin recording lasted 700 s with the fluorescence ratio $R_s < 32$ MΩ and with κ_S approximately constant. After

rupture of the patch, κ_S increased by 25% within 70 s. These experiments ($n = 4$) show that the nystatin pores are not permeable to Ca^{2+} binding anions as small as DA (molecular weight 132).

Intracellular fura-2: protein binding, accessible volume and photobleaching

From measurements of fluorescence emission anisotropy, Konishi, Olson, Hollingworth & Baylor (1989) concluded that up to 60–85% of intracellular fura-2 was bound by mobile intracellular proteins in skeletal muscle fibres, while in smooth muscle cells no such binding was found with the same method (Williams, Fogarty, Tsien & Fay, 1985).

In principle, intracellular protein binding of fura-2 will cause underestimation of $[B]_t$, and therefore also of κ_B and κ_S (see eqns (6)–(11)). To test for the existence of fura-2 binding to proteins, we measured the fluorescence from drops of internal solution (No. 2 in Table 1) in *n*-octanol (Reber & Reuter, 1991). It is expected that the F_i from a cell after equilibrium dialysis would be larger than that from drops of similar size, if there were a significant amount of fura-2 binding to intracellular proteins, and if a major part of the intracellular volume were accessible to fura-2. However, this is not the case. We formed cell-sized droplets in *n*-octanol at the tip of a pipette filled with fura-2 solution. The drop size was controlled by pressure applied to the pipette and was monitored by a CCD camera. During these measurements, the drops connected to the pipette tip were at equilibrium with fresh solution in the pipette which reduced photobleaching (see below). The pipettes were coated carefully with Sylgard nearly to the tip to facilitate forming fura-2 drops in the hydrophobic *n*-octanol. The F_i from 12 μm cells was only 29–51% of the fluorescence of microdroplets of the same size ($n = 8$). Although these experiments cannot exclude the existence of fura-2 binding sites, the present values may provide an upper bound for the accessible volume fraction of cytoplasmic fura-2.

During the course of these experiments, it was noticed that photobleaching of fura-2 drops in *n*-octanol was strikingly greater than in fura-2-loaded cells. In these experiments drops of internal solution with 70 μM fura-2 (No. 2 in Table 1) were separated from the application pipette and adhered to the chamber bottom. Their F_i signal decreased by 80% within 1000 s ($n = 5$). In contrast, the F_i signal in a cell preloaded with fura-2 to the same concentration (by a short whole-cell episode) decreased only 10% within 1000 s of continuous fluorescence measurement. In all our Ca^{2+} buffer experiments, within up to 400 s of nystatin recording, F_i decreased less than 4% due to bleaching. During whole-cell recordings the photobleaching should be negligible because bleached fura-2 is continuously exchanged for fresh fura-2 from the pipette. On average the time constant of fura-2 photobleaching in *n*-octanol was about 18 times shorter than that in cells.

DISCUSSION

Absence of highly mobile ligands

Comparing the Ca^{2+} binding capacity of cells during perforated recording with that during prolonged whole-cell recording we found no evidence for the presence of highly mobile Ca^{2+} binding sites. These would be expected to 'wash out' rapidly

when a patch is ruptured. On the other hand, adding a weakly Ca^{2+} binding organic anion, diglycolate, to the pipette solution does reveal 'wash-in' of its Ca^{2+} binding capacity after patch rupture. These findings show that relatively small changes in Ca^{2+} binding capacity can be detected, that a small organic anion does not equilibrate across a nystatin-perforated patch, and that there is no measurable Ca^{2+} binding capacity with high mobility. For the discussion below we assume an upper bound to the highly mobile Ca^{2+} binding capacity $\kappa_{S,m}$ ('m' for mobile) of 7. This amount, which is approximately the peak-to-peak noise in most of our recordings might have escaped detection.

Errors in estimating calcium binding capacity

Measurement of calcium binding capacity requires accurate measurement of the amount of calcium entering the cell ($\int I_{Ca}\,dt$) and of the fluorescence decrement. In addition, the calcium binding capacity of fura-2 has to be calculated for each measurement, which requires a knowledge of $[Ca^{2+}]_i$, of the concentration of fura-2, and of the dissociation constant of fura-2. All these quantities are subject to error. It is very important to have accurate calibration of fura-2 fluorescence and to use a dissociation constant of fura-2 compatible with this calibration (see Methods, eqn (2)). Furthermore inaccurate subtraction of background fluorescence, small amounts of photobleaching of fura-2 (Becker & Fay, 1987) or the presence of incompletely hydrolysed fura-2 ester can lead to gross underestimation of $[Ca^{2+}]_i$, and thereby overestimation of the calcium binding capacity of fura-2. Most of these sources of error are minimal when the cell is preloaded by a whole-cell pipette and when κ_B is approximately equal to κ_S, the endogenous binding capacity. Also, when trying to observe changes in κ_S it is advisable to design the experiment such that κ_B stays more or less constant (balanced loading, see Methods section) in order to keep the changes in errors to a minimum. Also, it is advisable to routinely check for indications of Ca^{2+} insensitive background fluorescence, such as saturation of Ca^{2+} signals at fluorescence ratio values lower than R_1, an apparent Ca^{2+} dependence of κ_S, and an apparent κ_S decay with a time constant characteristic for fura-2 during whole-cell recording (see Fig. 6*B*). Significant photobleaching of fura-2 during nystatin-patch recording may also cause this artifact. In our double whole-cell experiments, we did not observe this artifact, suggesting that photobleaching was small.

Besides these errors, which are the result of technical problems, there are more fundamental sources of error related to the calibration of the indicator dye. Comparing results given here with those given by Neher & Augustine (1992), one can see, that the present numbers are smaller by almost a factor of two. This reflects the fact that the present data are based on a fura-2 calibration using BAPTA, assuming a dissociation constant, $K_{d,BAPTA}$, under our conditions (0·160 M ionic strength, pH 7·2) of 225 nM. The previous work was based on an EGTA calibration, assuming $K_{d,EGTA}$ of 150 nM. Equations (6) and (9) show that κ values scale with the K_d of the indicator dye, which, in turn, scales inversely with the K_d assumed for the overall calibration. Thus, had we used the literature value of $K_{d,BAPTA}$ (given by Tsien, 1980) as 107 nM for 0·1 ionic strength) all our κ values would be larger by a factor of 2·5. However, BAPTA is very sensitive to ionic strength so that we performed the value given, which was calculated according to Harrison & Bers (1987). Also, binding of

fura-2 to cytoplasmic constituents (as discussed in the Results section) would influence the estimate for endogenous binding capacity, if bound fura-2 were still able to bind calcium.

Long-term measurements in the presence of intracellular nystatin

In artificial lipid membranes nystatin forms pores on either side of the membrane (Kleinberg & Finkelstein, 1984). It was thought that nystatin would also make pores from the inside of the plasma membrane if it was introduced into the cytoplasm (Rae & Fernandez, 1991). It has been reported that the whole-cell membrane becomes leaky after rupturing nystatin-permeabilized patches in lacrimal gland cells (Horn & Marty, 1988). In chromaffin cells, however, nystatin appears not to make pores from the inside of the plasma membrane. The reason for the discrepancy between results in different cell types might reside in the sterol requirement for nystatin pore formation (Cass & Finkelstein, 1970; Marty & Finkelstein, 1975; Horn & Marty, 1988).

Another interesting aspect of our measurements was that fura-2 seemed not to permeate through nystatin-permeabilized membranes. During prolonged nystatin-perforated-patch recording fura-2 was neither lost from an ester-loaded cell (in case the pipette did not contain fura-2) nor was there fura-loading (in which case the pipette had more fura-2 than the cell). This, of course, is not surprising in view of the finding that a much smaller Ca^{2+} binding anion (DA) does not permeate.

Poorly mobile buffers and diffusion in the presence of multiple buffers

Approximately half of the cells studied showed a Ca^{2+} binding capacity which decreased by 20–50% within about 500 s following patch rupture. This is indicative of mobile calcium binding sites in the molecular mass range 7–20 kDa (see Results section). These Ca^{2+} binding sites, like the fixed ones, appear to be of low affinity. Their contribution to Ca^{2+} binding capacity will be termed $\kappa_{s,s}$ ('s' for slow). Some of the known Ca^{2+} binding proteins meet these criteria, such as calmodulin (Feher, Fullmer & Fritzsch, 1989) and S-100β (Hilt & Kligman, 1991).

In order to discuss the contributions of different Ca^{2+} buffers to Ca^{2+} redistribution during recordings with a calcium indicator, such as fura-2, we consider four different Ca^{2+} ligands: (1) the Ca^{2+} indicator, such as fura-2, with Ca^{2+}-dependent binding capacity, κ_B, according to eqn (9), and a diffusion coefficient, D_b; (2) a highly mobile buffer with Ca^{2+} binding capacity, $\kappa_{s,m}$ ('m' for mobile), and diffusion coefficient, D_m; (3) a poorly mobile buffer with Ca^{2+} binding capacity, $\kappa_{s,s}$ ('s' for slow), and diffusion coefficient, D_s; and (4) a fixed buffer with Ca^{2+} binding capacity, $\kappa_{s,f}$ ('f' for fixed).

We include $\kappa_{s,m}$ although we have shown that it is small, in order to discuss bounds of its influence. The question we want to discuss is how these buffers interact in influencing the Ca^{2+} redistribution process following a perturbation. Of particular relevance is the influence of the Ca^{2+} indicator dye, fura-2.

We consider the total flux of calcium (bound or unbound), J_t, through a small volume element of width, Δx, which is given according to the law of diffusion by:

$$J_t = -\sum_{\nu} (D_\nu (dc_\nu/dx)), \tag{20}$$

where the sum extends over all Ca^{2+}-carrying chemical species (including Ca^{2+} itself) of concentration c_ν, and diffusion coefficients D_ν. For compatibility with the equations below the sum should formally also contain immobile buffers (with $D_\nu = 0$). According to the definition of calcium binding capacities, such as eqn (5), we have

$$\kappa_\nu = \mathrm{d}c_\nu/\mathrm{d}[Ca^{2+}]_i. \tag{21}$$

Equation (20) can be written for small excursions in $[Ca^{2+}]_i$ from steady state, assuming local equilibrium between $[Ca^{2+}]_i$ and its ligands:

$$J_t = -(\mathrm{d}[Ca^{2+}]_i/\mathrm{d}x)\,\Sigma(\kappa_\nu D_\nu). \tag{22}$$

With the total concentration of calcium $[Ca]_t$ given by

$$[Ca]_t = \Sigma c_\nu, \tag{23}$$

and eqn (21), assuming spatial uniformity of total buffer concentrations, we have

$$\mathrm{d}[Ca]_t/\mathrm{d}x = \Sigma(\mathrm{d}c_\nu/\mathrm{d}x) = (\mathrm{d}[Ca^{2+}]_i/\mathrm{d}x)\,\Sigma\kappa_\nu. \tag{24}$$

Inserting eqn (24) into eqn (22) we obtain

$$J_t = -(\mathrm{d}[Ca]_t/\mathrm{d}x)\,(\Sigma(\kappa_\nu D_\nu))/(\Sigma\kappa_\nu). \tag{25}$$

This equation describes the law of diffusion for the flux of total calcium in terms of an 'effective diffusion coefficient', D', which is given by

$$D' = (\Sigma(\kappa_\nu D_\nu))/(\Sigma\kappa_\nu). \tag{26}$$

For small excursions D' also describes the diffusion of free calcium. Here the sum is extended over all chemical species which carry calcium, including calcium itself ($\kappa_{Ca} = 1$). Formally, fixed buffers are included with the corresponding D_ν equal to zero. It should be emphasized that κ values depend on $[Ca^{2+}]_i$ and that, unless this is specifically taken into account, this simplified law of diffusion holds only for Ca^{2+} changes which are small with respect to the dissociation constants of the buffers involved. Also, it holds only for changes which proceed slower than the relaxation times for all the binding–unbinding reactions involved.

Considering free calcium, and the buffer species mentioned above we obtain:

$$D' = \frac{D_{Ca} + D_m\kappa_{S,m} + D_s\kappa_{S,s} + D_b\kappa_B}{1 + \kappa_{S,m} + \kappa_{S,s} + \kappa_{S,f} + \kappa_B}, \tag{27}$$

where κ_B is a function of $[Ca^{2+}]_i$ (eqn (9)), whereas all other quantities are constant within the range 0·1–2 μM.

In order to estimate the effective diffusion coefficient D' or, more specifically, the contribution to D' of a given ligand of calcium, all eight parameters of eqn (27) have to be known. Table 3 lists numerical values for the quantities of eqn (27), as derived in the Results section or as taken from the literature. The concentration of fura-2 ([fura-2]) was assumed to be 50 μM, and the concentration of calcium 240 nM. It is seen (last column of Table 3) that even for very little fura-2, its contribution is the dominating term in the numerator of eqn (27). It is also apparent that the contribution of the poorly mobile buffer is very small, about half of that of free

calcium. In the absence of fura-2 the term for highly mobile buffer, which must be considered an upper bound to the true value, is dominating. In order to show the influence of fura-2, the effective diffusion coefficient, D', is plotted *versus* [fura-2] for different cases in Fig. 8 (see legend). In all cases D' approaches the value for fura-2 diffusion (D_b) in the limit of high [fura-2]. In Fig. 8*A*, D_b was set to the value given

TABLE 3. Effective diffusion coefficient of Ca-ligands

	Diffusion coefficient		Ca^{2+} binding capacity		
Species	Symbol	Value ($cm^2\ s^{-1}$)	Symbol	Value	Product ($\kappa_y D_y$) ($\times 10^{-6}\ cm^2\ s^{-1}$)
Calcium	D_{Ca}	3×10^{-6} [a]	—	1	3
Fura-2	D_b	4×10^{-7} [b]	κ_B	52 [e]	21
Highly mobile buffer	D_m	2×10^{-6} [c]	$\kappa_{S,m}$	7 [f]	14
Poorly mobile buffer	D_s	$1{\cdot}5 \times 10^{-7}$ [d]	$\kappa_{S,s}$	9 [g]	1·3
Fixed buffer	—	0	$\kappa_{S,f}$	32 [h]	0

[a] Half the value of free aqueous diffusion, to allow for effects of tortuosity and viscosity, as observed for other small ions (Kushmerick & Podolsky, 1969).
[b] Timmerman & Ashley, 1986.
[c] Half the value of a molecule of molecular mass = 500 Da.
[d] Diffusion coefficient of fura-2 multiplied by the ratio of dialysis time constants.
[e] Value calculated for 50 μM fura-2 and 0·24 μM calcium according to eqn (9).
[f] Upper bound for mobile buffer, as given in Results section.
[g] Mean of poorly mobile buffer, as given in Discussion.
[h] Total buffer, as given in Results section, minus poorly mobile buffer.

by Timmermann & Ashley (1986), as measured in muscle cells. In the presence of highly mobile buffer (upper two curves in Fig. 8*A*) the variation in D' with [fura-2] is, in fact, quite small because the starting value (in the absence of fura-2) incidentally is quite close to the diffusion coefficient of fura-2. A choice of D_m somewhat higher would even predict D' to be a decaying function of [fura-2]. In the absence of highly mobile buffer, however, D' changes quite markedly from $0{\cdot}1 \times 10^{-6}\ cm^2\ s^{-1}$ to about $0{\cdot}4 \times 10^{-6}\ cm^2\ s^{-1}$. A much stronger influence of fura-2 is predicted if its diffusion coefficient is assumed to be higher. Preliminary measurements in snail neurons (M. Spira, personal communication) indicate that, contrary to the case of muscle cells, the value may be as large as $1{\cdot}7 \times 10^{-6}\ cm^2\ s^{-1}$. This would be close to the diffusion coefficient of other BAPTA derivatives found by Adler, Augustine, Duffy & Charlton (1991). In Fig. 8*B* the predictions for the effective diffusion coefficient of calcium (D') are shown for $D_b = 1{\cdot}7 \times 10^{-6}\ cm^2\ s^{-1}$. D_s was set to $0{\cdot}63 \times 10^{-6}\ cm^2\ s^{-1}$ in order to keep the ratio D_b/D_s constant. All other parameters are the same as in Fig. 8*A*. It is seen that under these assumptions as little [fura-2] as 10 μM more than doubles the effective diffusion coefficient in most situations. Comparing *A* and *B* of Fig. 8 emphasizes the important influence of the mobility of an indicator dye on the Ca^{2+} measurement.

The true value of $\kappa_{S,m}$ is not known. The value assumed in Table 3 and Fig. 8 is an upper bound which we might have detected, if it had been present. On the other hand, the presence of metabolites definitely provides some background of mobile Ca^{2+} buffers. J. Kleineke & H. D. Söling (personal communication) estimated calcium

bound to metabolites in the cytosol of rat liver cells. They concluded that ATP was the main ligand for calcium in the cytosol, being present at a total concentration of 2·6 mM. They also estimated free [Mg^{2+}] to be 0·47 mM. Given a pK (−log of dissociation constant) for the Mg–ATP complex of 4·06 (Smith & Martell, 1975) and

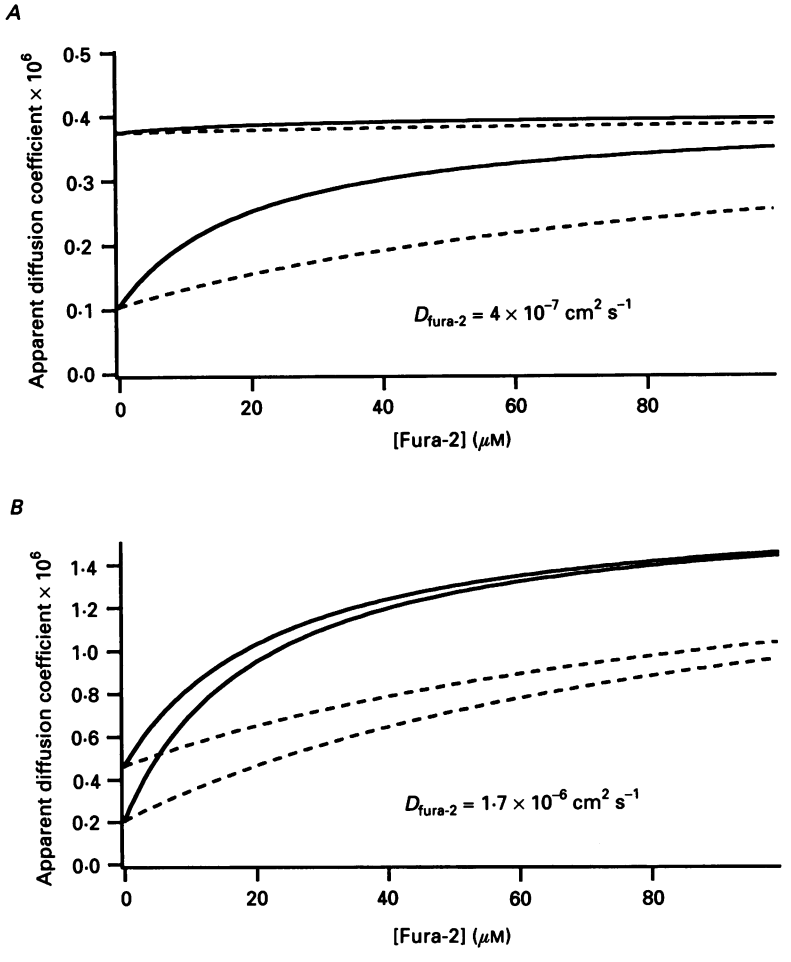

Fig. 8. The apparent diffusion coefficient, D', as a function of fura-2 concentration. A, D' was evaluated according to eqn (27) assuming a fura-2 diffusion coefficient of $0{\cdot}4 \times 10^{-6}$ cm^2 s^{-1}. For the upper two curves a highly mobile buffer, $\kappa_{s,m}$, of 7 was assumed, which is considered to be an upper bound. The continuous line holds for a Ca^{2+} concentration of 0·1 μM, the dashed line for 0·5 μM. The lower two curves are analogous to the upper ones, but in the absence of highly mobile buffers ($\kappa_{s,m} = 0$). B, same as A, but using a fura-2 diffusion coefficient of $1{\cdot}7 \times 10^{-6}$ cm^2 s^{-1} and D_s of $0{\cdot}63 \times 10^{-6}$ cm^2 s^{-1}. Note different Y-axis scaling in A and B.

assuming that most of the ATP not complexed with Mg^{2+} is free, one would expect free [ATP] to be 0·4 mM. This is twice the dissociation constant of the Ca–ATP complex (Smith & Martell, 1975). Thus, ATP alone is capable of contributing a value

of 2 to $\kappa_{S,m}$. With this, a lower bound to D' at zero fura-2 of $0{\cdot}19 \times 10^{-6}$ cm^2 s^{-1} is obtained. Thus, values around $0{\cdot}2 \times 10^{-6}$ cm^2 s^{-1} should hold unless Ca^{2+} diffusion is dominated by that of the fura-2 complex. These values are somewhat lower than the ones given by Nasi & Tillotson (1985) for *Aplysia* cytoplasm ($0{\cdot}83 \times 10^{-6}$ cm^2 s^{-1}) and by Hodgkin & Keynes (1957) for squid axoplasm ($0{\cdot}6 \times 10^{-6}$ cm^2 s^{-1}). They are close to the value found for myoplasm ($0{\cdot}14 \times 10^{-6}$ cm^2 s^{-1}) by Kushmerick & Podolsky (1969). It should be stressed, however, that these values are not exactly comparable. The earlier data, particularly those based on tracer fluxes, measured diffusional spread in time spans of minutes, during which calcium can equilibrate with sequestering organelles. The value by Nasi & Tillotson (1985) may contain a contribution from calcium bound to arsenazo.

The above discussion points towards a number of criteria that must be met for a realistic measurement of the effective diffusion coefficient of calcium. (i) The measurement has to take place in a time span less than 1 s. Otherwise Ca^{2+} sequestration mechanisms participate (see also Neher & Augustine, 1992). (ii) Free calcium during the measurement should not exceed 2 μM, because constancy of endogenous buffer capacity has only been ascertained in that range. (iii) When using fura-2 the influence of the dye is best seen in the concentration range 5–50 μM (see Fig. 8). In order to obtain values representative of the unperturbed cell, an extrapolation towards zero [fura-2] would be necessary. To our knowledge no measurements meeting all these criteria are available at the moment.

APPENDIX A

At $f = f_{max}/2$, κ_S in eqn (6) has its lowest error sensitivity with respect to f

With presumption of $\kappa_S \gg 1$, let us define $g(f)$, the relative error in κ_S:

$$g(f) = (\kappa_S(f+\Delta f) - \kappa_S(f))/\kappa_S(f) = -\Delta f f_{max}/(f(f_{max} - f)), \tag{A1}$$

where Δf is a small increment of f. To get the minimum $g(f)$, the condition

$$g'(f) = 0, \tag{A2}$$

where $g'(f)$ is the derivative of $g(f)$, should be fulfilled. From eqns (6), (A1) and (A2) we obtain $f = f_{max}/2$. At this value the relative error is $4 \times \Delta f/f_{max}$. If the relative error $\Delta f/f_{max}$ is 5%, then $g(f)$ is 56, 31, 20, 31 and 56% for values of $f/f_{max} = 0{\cdot}1$, $0{\cdot}2$, $0{\cdot}5$, $0{\cdot}8$ and $0{\cdot}9$, respectively.

APPENDIX B

Derivation of eqn (19)

From eqn (13),

$$F_2 = F_{2e} + F_{2b}. \tag{A3}$$

It is assumed that all of the Ca^{2+}-sensitive fura-2 is saturated immediately following the injection of calcium due to an appropriate depolarizing pulse. At this time $F_x = F_{xs}$, where the subscript 'x' stands for 350 or 390 nm and the subscript 's' for 'fura-2-saturated state'. Because the calibration parameter R_1 in eqn (1) is

$$R_1 = F_{1se}/F_{2se}, \tag{A4}$$

we obtain from eqns (12) and (13)

$$F_{ise} = (1-r_2)F_{is}. \tag{A5}$$

From eqns (A3)–(A5), (12) and (14) we have

$$F_{2s} = (1-r_2)F_{is}/R'_1 + r_2 F_{is}/R'_b, \tag{A6}$$

$$r_2 = (1-R'_1(F_{2s}/F_{is}))/(1-R'_1/R'_b), \tag{A7}$$

which yields eqn (19) with $R'_s = F_{is}/F_{2s}$.

APPENDIX C

Derivation of r_3

Suppose that pulse 1 induces a small Ca^{2+} influx, and pulse 2 induces a larger Ca^{2+} influx. According to the presumptions for r_3 and eqns (6), (10) and (16) we have

$$\kappa_{S1e} = \kappa_{B1e}(f_{max}/f_1 - 1) - 1, \tag{A8}$$

$$\kappa'_{B1e} = \frac{[B]_t}{K_d(1+[Ca^{2+}]_{a1}/K_d)(1+[Ca^{2+}]_{b1}/K_d)}, \tag{A9}$$

$$\kappa_{S2e} = \kappa_{B2e}(f_{max}/f_2 - 1) - 1, \tag{A10}$$

$$\kappa_{B2e} = \frac{[B]_t}{K_d(1+[Ca^{2+}]_{a2e}/K_d)(1+[Ca^{2+}]_{b2}/K_d)}, \tag{A11}$$

where κ_{S1e}, κ_{B1e}, κ_{S2e}, and κ_{B2e} are true values of κ_S and κ_B during pulse 1 and pulse 2 respectively. $[Ca^{2+}]_{a2e}$ is the true peak value of $[Ca^{2+}]_i$ after pulse 2. From eqns (1) and (16),

$$[Ca^{2+}]_{a2e} = -K_{eff}(s_0 + r_3 t_0)/(s_1 + r_3 t_1), \tag{A12}$$

$$s_0 = 1 - R'_0/R'_{a2}, \tag{A13}$$

$$s_1 = 1 - R'_1/R'_{a2}, \tag{A14}$$

$$t_0 = R'_0/R'_b - 1, \tag{A15}$$

$$t_1 = R'_1/R'_b - 1, \tag{A16}$$

where R'_{a2} is the value of R' after pulse 2. From the presumption we have

$$\kappa_{S1e} = \kappa_{S2e}. \tag{A17}$$

From eqns (A8)–(A17),

$$r_3 = \frac{s_1(1-n) - s_0 K_{eff}/K_d}{t_0 K_{eff}/K_d - t_1(1-n)}, \tag{A18}$$

$$n = \frac{[B]_t(f_{max}/f_2 - 1)}{K_d \kappa_{B1}(f_{max}/f_1 - 1)(1+[Ca^{2+}]_{b2}/K_d)}. \tag{A19}$$

APPENDIX D

A method for κ_S estimation without f_{max}

Sala & Hernandez-Cruz (1990) have suggested that it may be possible to detect κ_S by a difference in Ca^{2+} affinity between dye and endogenous buffer. In chromaffin cells, we have concluded that the Ca^{2+} affinity of the endogenous buffers are much smaller than that of fura-2 (see Results).

Here we provide a method for measuring κ_S which does not require that the parameter f_{max} has to be determined in a separate experiment. The fura-2 fluorescence and whole-cell Ca^{2+} currents are monitored in response to two depolarizing pulses with significantly different durations. This method is based on the assumption that κ_S is the same for each of the two depolarization-induced $[Ca^{2+}]_i$ spikes.

The increment of intracellular calcium immediately after a depolarizing pulse is

$$\Delta[Ca]_t = h\int I_{Ca}\,dt, \tag{A20}$$

where h is constant. $\int I_{Ca}\,dt$ is the integral of whole-cell Ca^{2+} current during the depolarizing pulse.

From eqns (4) and (5) and the definition of κ'_B we have

$$\Delta[Ca]_t = \Delta[Ca^{2+}]_i(1+\kappa_S+\kappa'_B). \tag{A21}$$

From eqns (A20) and (A21), with pulse 1 and pulse 2 we have

$$\Delta[Ca^{2+}]_{i1}(1+\kappa_{S1}+\kappa'_{B1}) = h\int I_{Ca1}\,dt, \tag{A22}$$

$$\Delta[Ca^{2+}]_{i2}(1+\kappa_{S2}+\kappa'_{B2}) = h\int I_{Ca2}\,dt, \tag{A23}$$

where $[Ca^{2+}]_{i1}$, $[Ca^{2+}]_{i2}$, κ_{S1}, κ_{S2}, κ'_{B1}, κ'_{B2}, $\int I_{Ca1}\,dt$ and $\int I_{Ca2}\,dt$ are $[Ca^{2+}]_i$, κ_S, κ'_B and $\int I_{Ca}\,dt$ after pulse 1 and pulse 2, respectively. Assuming that κ_S is constant throughout, we have

$$\kappa_S = \kappa_{S1} = \kappa_{S2}, \tag{A24}$$

$$\kappa_S = \frac{m(1+\kappa'_{B2})-(1+\kappa'_{B1})}{1-m}, \tag{A25}$$

$$m = \frac{\int I_{Ca1}\,dt \times \Delta[Ca^{2+}]_{i2}}{\int I_{Ca2}\,dt \times \Delta[Ca^{2+}]_{i1}}. \tag{A26}$$

These equations cannot be applied to data from pulses during wash-out of the mobile Ca^{2+} buffers because then the condition of constant κ_S is violated. However, they are valid for data from nystatin-patch recording or from whole-cell measurements after complete wash-out of mobile endogenous calcium buffers.

To obtain an accurate κ_S estimation from eqn (A25), the following criteria must be fulfilled. (1) The $[Ca^{2+}]_i$ measurement must be accurate. (2) The $\int I_{Ca}\,dt$ measurement must be accurate. (3) Let $m > 1{\cdot}5$. This is generally the case, if $[B]_t$ is not too large and if durations of the two pulses are significantly different. With $[B]_t = 70\ \mu M$, and with pulse 1 and pulse 2 having durations of 20 and 50 ms, respectively, m is about 1·5–3·5, and κ_S estimated by eqn (A25) is nearly identical to κ_S estimated from eqn (6).

APPENDIX E

The isocoefficient

Let S_{f1}, S_{b1}, S_{f2} and S_{b2} be the specific fluorescence intensities of the free (f) and bound (b) form of fura-2, for the wavelengths 1 and 2, respectively, as defined by Grynkiewicz *et al.* (1985). Then fluorescence values F_1 and F_2 can be written as

$$F_1 = S_{f1} n_f + S_{b1} n_b, \tag{A27}$$

$$F_2 = S_{f2} n_f + S_{b2} n_b, \tag{A28}$$

where n_b and n_f are the molar quantities of bound and free fura-2, respectively. With these definitions the parameters of the calibration formula for fura-2 (eqn (1)) are:

$$R_0 = S_{f1}/S_{f2}, \tag{A29}$$

$$R_1 = S_{b1}/S_{b2}, \tag{A30}$$

$$K_{eff} = K_d S_{f2}/S_{b2}, \tag{A31}$$

During a change in $[Ca^{2+}]_i$ conservation of fura-2 requires that

$$\Delta n_f = -\Delta n_b. \tag{A32}$$

We look for an 'isocoefficient', α, such that

$$\Delta(F_1 + \alpha F_2) = 0, \tag{A33}$$

$$= \Delta n_f (S_{f1} + \alpha S_{f2}) + \Delta n_b (S_{b1} + \alpha S_{b2}).$$

With eqn (A32) this leads to

$$\alpha = (S_{b1} - S_{f1})/(S_{f2} - S_{b2}). \tag{A34}$$

With eqns (A29)–(A30), the expression for α (eqn (A34)) can be written:

$$\alpha = (R_1 S_{b2}/S_{f2} - R_0)/(1 - S_{b2}/S_{f2}). \tag{A35}$$

From this

$$S_{b2}/S_{f2} = (\alpha + R_0)/(\alpha + R_1), \tag{A36}$$

and with eqn (A31) we get

$$K_d = K_{eff} S_{b2}/S_{f2} = K_{eff}(\alpha + R_0)/(\alpha + R_1).$$

We thank R. H. Chow, L. von Rüden, S. H. Heinemann, M. C. Nowycky, M. J. Pinter and R. S. Zucker for critical reading and helpful suggestions on the manuscript and M. Pilot for cell preparation. We also thank J. Kleineke and H. D. Söling, University of Göttingen, for supplying unpublished material on cytoplasmic constituents, and M. Spira, Hebrew University, Jerusalem, for information on the fura-2 diffusion coefficient in snail neurons.

REFERENCES

ADLER, E. M., AUGUSTINE, G. J., DUFFY, S. N. & CHARLTON, M. P. (1991). Alien intracellular calcium chelators attenuate neurotransmitter release at the squid giant synapse. *Journal of Neuroscience* **11**, 1496–1507.

AHMED, Z. & CONNOR, J. A. (1988). Calcium regulation by and buffer capacity of cell calcium. *Cell Calcium* **9**, 57–69.

ARTALEJO, C. R., MOGUL, D. J., PERLMAN, R. L. & FOX, A. P. (1991). Three types of bovine chromaffin cell Ca^{2+}-channels: facilitation increases the opening probability of a 27 pS channel. *Journal of Physiology* **444**, 213–240.

AUGUSTINE, G. J. & NEHER, E. (1992). Neuronal Ca^{2+} signalling takes the local route. *Current Opinion in Neurobiology* **2**, 302–307.

BAYLOR, S. M., HOLLINGWORTH, S. & KONISHI, M. (1989). Calcium transients in intact frog single skeletal muscle fibres measured with the fluorescence indicator dye Mag-fura-2. *Journal of Physiology* **419**, 69*P*.

BECKER, P. L. & FAY, F. S. (1987). Photobleaching of fura-2 and its effect on determination of calcium concentrations. *American Journal of Physiology* **253**, C613–618.

BEZANILLA, F. & ARMSTRONG, C. M. (1977). Inactivation of the sodium channel. (I). Sodium current experiments. *Journal of General Physiology* **70**, 549–566.

CASS, A. & FINKELSTEIN, A. (1970). The ion permeability induced in thin lipid membranes by the polyene antibiotics nystatin and amphotericin B. *Journal of General Physiology* **56**, 100–124.

ECKERT, R. & CHAD, J. E. (1984). Inactivation of Ca channels. *Progress in Biophysics and Molecular Biology* **44**, 215–267.

FEHER, J. J., FULLMER, C. S. & FRITZSCH, G. K. (1989). Comparison of the enhanced steady-state diffusion of calcium by calbindin-D9K and calmodulin: possible importance in intestinal calcium absorption. *Cell Calcium* **10**, 189–203.

FENWICK, E. W., MARTY, A. & NEHER, E. (1982*a*). A patch clamp study of bovine chromaffin cells and of their sensitivity to acetylcholine. *Journal of Physiology* **331**, 577–597.

FENWICK, E. M., MARTY, A. & NEHER, E. (1982*b*). Sodium and calcium channels in bovine chromaffin cells. *Journal of Physiology* **331**, 599–635.

GORMAN, A. L. F. & THOMAS, M. V. (1980). Intracellular calcium accumulation during depolarization in a molluscan neurone. *Journal of Physiology* **308**, 259–285.

GRYNKIEWICZ, G., POENIE, M. & TSIEN, R. Y. (1985). A new generation of Ca^{2+} indicators with greatly improved fluorescence properties. *Journal of Biological Chemistry* **260**, 3440–3450.

HAMILL, O. P., MARTY, A., NEHER, E., SAKMANN, B. & SIGWORTH, F. J. (1981). Improved patch-clamp techniques for high-resolution current recording from cells and cell-free membrane patches. *Pflügers Archiv* **391**, 95–100.

HARRISON, S. M. & BERS, D. M. (1987). The effect of temperature and ionic strength on the apparent Ca-affinity of EGTA and the analogous Ca-chelators BAPTA and dibromo-BAPTA. *Biochimica et Biophysica Acta* **925**, 133–143.

HILT, D. C. & KLIGMAN, D. (1991). The S-100 protein family: a biochemical and functional overview. In *Novel Calcium-binding Proteins*, ed. HEIZMANN, C. W., pp. 65–103. Springer, Berlin.

HODGKIN, A. L. & KEYNES, R. D. (1957). Movements of labelled calcium in squid giant axons. *Journal of Physiology* **138**, 253–281.

HORN, R. & KORN, S. J. (1992). Prevention of rundown in electrophysiological recording. In *Methods in Enzymology*, vol. 207, ed. RUDY, B. & IVERSON, L. E., pp. 149–155. Academic Press, New York.

HORN, R. & MARTY, A. (1988). Muscarinic activation of ionic currents measured by a new whole-cell recording method. *Journal of General Physiology* **92**, 145–159.

KLEINBERG, M. E. & FINKELSTEIN, A. (1984). Single-length and double-length channels formed by nystatin in lipid bilayer membranes. *Journal of Membrane Biology* **80**, 257–269.

KONISHI, M., OLSON, A., HOLLINGWORTH, S. & BAYLOR, S. M. (1989). Myoplasmic binding of fura-2 investigated by steady-state fluorescence and absorbance measurement. *Biophysical Journal* **54**, 1089–1104.

KUSHMERICK, M. J. & PODOLSKY, R. J. (1969). Ionic mobility in muscle cells. *Science* **166**, 1297–1298.

MCBURNEY, R. N. & NEERING, V. (1985). The measurement of changes in intracellular free calcium during action potentials in mammalian neurones. *Journal of Neuroscience Methods* **13**, 65–76.

MARTY, A. & FINKELSTEIN, A. (1975). Pores formed in lipid bilayer membranes by nystatin: differences in its one-sided and two-sided action. *Journal of General Physiology* **65**, 515–526.

MARTY, A. & NEHER, E. (1983). Tight-seal whole-cell recording. In *Single Channel Recording*, ed. SAKMANN, B. & NEHER, E., pp. 107–122. Plenum Press, New York.

MARTY, A. & NEHER, E. (1985). Potassium channels in cultured bovine adrenal chromaffin cells. *Journal of Physiology* **367**, 117–141.

NASI, E. & TILLOTSON, D. (1985). The rate of diffusion of Ca^{2+} and Ba^{2+} in a nerve cell body. *Biophysical Journal* **47**, 735–738.

NEHER, E. (1989). Combined fura-2 and patch clamp measurements in rat peritoneal mast cells. In *Neuromuscular Junction*, ed. SELLIN, L. C., LIBELIUS, R. & THESLEFF, S., pp. 65–76. Elsevier, Amsterdam.

NEHER, E. (1992). Correction for liquid junction potentials in patch clamp experiments. *Methods in Enzymology* **207**, 123–131.

NEHER, E. & AUGUSTINE, G. J. (1992). Calcium gradients and buffers in bovine chromaffin cells. *Journal of Physiology* **450**, 273–301.

NOWYCKY, M. C. & PINTER, J. (1993). Time courses of calcium and calcium bound buffers following calcium influx in a model cell. *Biophysical Journal* **64**, 77–91.

PUSCH, M. & NEHER, E. (1988). Rates of diffusional exchange between small cells and a measuring patch pipette. *Pflügers Archiv* **411**, 204–211.

RAE, L., COOPER, K., GATES, P. & WATSKY, M. (1991). Low access resistance perforated patch recording using amphotericin B. *Journal of Neuroscience Methods* **37**, 15–26.

RAE, J. L. & FERNANDEZ, J. (1991). Perforated patch recordings in physiology. *News in Physiological Sciences* **6**, 273–275.

REBER, B. F. X. & REUTER, H. (1991). Dependence of cytosolic calcium in differentiating rat pheochromocytoma cells on calcium channels and intracellular stores. *Journal of Physiology* **435**, 145–162.

SALA, F. & HERNANDEZ-CRUZ, A. (1990). Calcium diffusion modeling in a spherical neuron – relevance of buffering properties. *Biophysical Journal* **57**, 313–324.

SCANLON, M., WILLIAMS, D. A. & FAY, F. S. (1987). A Ca^{2+}-insensitive form of fura-2 associated with polymorphonuclear leukocytes. *Journal of Biological Chemistry* **262**, 6308–6312.

SMITH, R. M. & MARTELL, A. E. (1975). *Critical Stability Constants*, vol. 2. Plenum Press, New York.

SMITH, S. & ZUCKER, R. (1980). Aequorin response facilitation and intracellular calcium accumulation in molluscan neurones. *Journal of Physiology* **300**, 167–196.

TIMMERMAN, M. P. & ASHLEY, C. C. (1986). Fura-2 diffusion and its use as an indicator of transient free calcium changes in single striated muscle cells. *FEBS Letters* **209**, 1–8.

TSIEN, R. Y. (1980). New calcium indicators and buffers with high selectivity against magnesium and protons: design, synthesis, and properties of prototype structures. *Biochemistry* **19**, 2396–2404.

WILLIAMS, D. A., FOGARTY, K. E., TSIEN, R. Y. & FAY, Y. S. (1985). Calcium gradients in single smooth muscle cells revealed by the digital imaging microscope using Fura-2. *Nature* **318**, 558–561.

ZHOU, Z. & NEHER, E. (1992). Mobile Ca^{2+} buffers in bovine adrenal chromaffin cells. *Biophysical Journal* **61**, A124.